JMEPEG (2012) 21:1313–1319
DOI: 10.1007/s11665-011-0048-4

1059-9495/$19.00

Heat Strength Evaluation and Microstructures Observation of the Welded Joints of One China-Made T91 Steel

Yi Gong, Zhen-Guo Yang, and Fa-Yun Yang

(Submitted December 8, 2010; in revised form May 16, 2011)

T91 (9Cr1MoVNb), the martensitic heat-resistant steel, is widely applied in industries like power generation, petrochemical, nuclear, etc., and a wealth of researches has been conducted on its properties so far. However, actually for China, T91 was begun to be domestically manufactured only from the end of last century. Hence, thorough assessments of the China-made T91 steels are always urgently required, especially for its welded joints. In this paper, the relationship between mechanical properties and microstructures of the welded joints of one China-made T91 steel was experimentally discussed. Moreover, aging test and creep rupture test were utilized for both analyzing the heat strength and predicting the service life of the joints. Results showed that welded joints of this China-made T91 steel could exhibit sufficient strength under the operating conditions of most nuclear reactors used nowadays.

Keywords Creep rupture, Microstructure, T91, Welded joints

1. Introduction

Although it has been mainly applied as the matrix material for steam tubes of superheaters, reheaters, etc., in supercritical (SC) and/or ultra-supercritical (USC) plants in power generation industry for over 30 years, T91 (9Cr1MoVNb), the martensitic heat-resistant steel, is still one of the most frequently used structural materials in nuclear industry (Ref 1, 2). The original aim of developing T91 by ORNAL and CE in 1970s was just for liquid metal fast breeder reactors (LMFBR) (Ref 3, 4). Actually, owing to the increasing steam parameters in next generation USC plants (above 625 °C, 30 MPa) for the purpose of higher fuels utilization and lower CO_2 emission (Ref 5, 6), T91 is now gradually substituted by novel martensitic heat-resistant steels with even superior high temperature properties, such as T92 (9Cr0.5Mo1.8WVNb), T911 (9Cr1Mo1WNb), T122 (12Cr0.5Mo2WCuVNb), and so on (Ref 7–11). However, as the steam parameters are not as severe as that in USC plants, also considering its mature service experiences and high performance versus price ratio, T91 will certainly maintain its popularity in the foreseeable future in nuclear power plants, which are always attracting the incentive drives from the governments all over the world.

In the past two decades, a great deal of researches has been carried out on the mechanical properties (Ref 12, 13), corrosion resistance (Ref 14–16), creep performances (Ref 17–19), and microstructures evolution (Ref 20–23) of this familiar material at elevated temperatures, even exposed to the nuclear environments (Ref 24, 25). With respect to the similar and/or the dissimilar welded joints of it, Das and co-workers (Ref 26, 27) analyzed the relationship between mechanical properties and microstructures, Thomas (Ref 28) investigated the residual stresses after welding, Spigarelli (Ref 29) studied the creep rate, and Li and co-workers (Ref 30, 31, 32) evaluated the creep rupture properties and predicted the service lives. However, in fact, T91 was not imported into China until the beginning of the 90s in last century, and was started to be domestically made only from the end of last century. Thus, comprehensive assessment of the China-made T91 steels and their welded joints plays a critical role in popularizing them in engineering practice, even supporting the national industry of China.

In this paper, study mainly accumulated in the welded joints that were produced by a kind of China-made T91 steel. In order to discuss the relationship between mechanical properties and microstructures, tensile tests were carried out at both room and increasing temperatures on the welded joints, while optical microscope (OM) and transmission electron microscope (TEM) were utilized to observe the metallographic microstructures and the carbides precipitation across the joints, particularly in the heat-affected zone (HAZ) and the weld seam. Furthermore, at 625 °C, not only the aging test was conducted to evaluate the performance deterioration of the joints, but also the creep rupture test was employed to predict their service lives. Achievements of this paper supplemented relevant heat strength data of T91 welded joints for engineering practice, and could also provide solid foundation for popularization of this China-made T91 steel in the nuclear industry.

2. Experimental

Tested materials were nominal T91 heat-resistant steels with scale of 47.6OD × 7 mm thick. Chemical compositions and

Yi Gong, and **Zhen-Guo Yang**, Department of Materials Science, Fudan University, Shanghai 200433, People's Republic of China; **Fa-Yun Yang**, Power Station, Baosteel Group Co. Ltd., Shanghai 201900, People's Republic of China. Contact e-mail: zgyang@fudan.edu.cn.

heat treatment conditions of them are listed in Table 1, which are in accordance with the requirements of ASME SA-213 T91 specifications (Ref 33). As is shown in Fig. 1(a), no obvious coarse nonmetallic inclusions were present in the material (Ref 34). Furthermore, etched in agent of picric acid (2,4,6-trinitrophenol) 1.25 g, HCl 20 mL, ethanol 10 mL, and H_2O 10 mL for 40 s, its metallographic microstructure is shown in Fig. 1(b), which displays a typical tempered lath martensitic microstructure with average lath width of about 1 μm.

The T91 welded joints were welded by means of gas tungsten arc welding (GTAW) with pure argon gas (Ar) as the shielding gas and AWS ER90S-B9 as the welding wire (Φ 1.0 mm), whose chemical compositions are listed in Table 2 (Ref 35). The welding current and voltage were, respectively, 230 A and 14 V, and the number of weld passes was three. Then, the joints were subjected to the post-weld heat treatment (PWHT) at 730-760 °C for 1 h to eliminate the residual stresses.

A variety of mechanical tests for the welded joints were also successively carried out. Tensile test and bending test were performed at room temperature according to the ASTM E8-04 (Ref 36) and E290-97a(2004) (Ref 37) standards. Also, tensile properties of the joints were evaluated at increasing temperatures from 50 to 650 °C with increment of 50 °C based on ISO 783-1999 (Ref 38) standard. Metallographic microstructures and carbides evolution across the welded joints before and after welding, especially in the HAZ and the weld seam, were then inspected, respectively, under LEICA DMLM optical microscope and PHILIPS EM 430 TEM. Finally, in accordance with ASTM E139-06 (Ref 39) standard, creep rupture test was conducted at 625 °C under load stresses from 65 to 150 MPa with increment of 5 or 10 MPa. Meanwhile, high temperature aging test was achieved on the welded joints at this temperature as well.

3. Results and Discussion

3.1 Mechanical Properties at Room and Increasing Temperatures

It can be learned from Table 3 that the T91 welded joints exhibited qualified tensile strength according to the T91 base material specification, only the elongation was a bit lower. Table 4 reveals that the welded joints also presented eligible toughness, and no cracks were found on the bended surfaces.

Table 5 and Fig. 2 show the tensile properties of the T91 welded joints at increasing temperatures. Compared with the requirements of T91 base material in GB 5310 standard of

Table 1 Chemical compositions and heat treatment conditions of the T91 sample (wt.%)

Elements	C	Mn	P	S	Si	Cr	Mo	V	Nb	N	Ni	Al
T91 Sample	0.09	0.41	0.011	0.002	0.29	8.82	0.90	0.20	0.08	0.040	0.12	0.013
ASME SA-213 T91	0.08–0.12	0.30-0.60	≤0.020	≤0.010	0.20-0.50	8.00-9.50	0.85-1.05	0.18-1.05	0.06-0.10	0.030-0.070	≤0.40	≤0.04

Heat treatment conditions: 1060 °C × 20 min (normalizing) + 780 °C × 60 min (tempering)

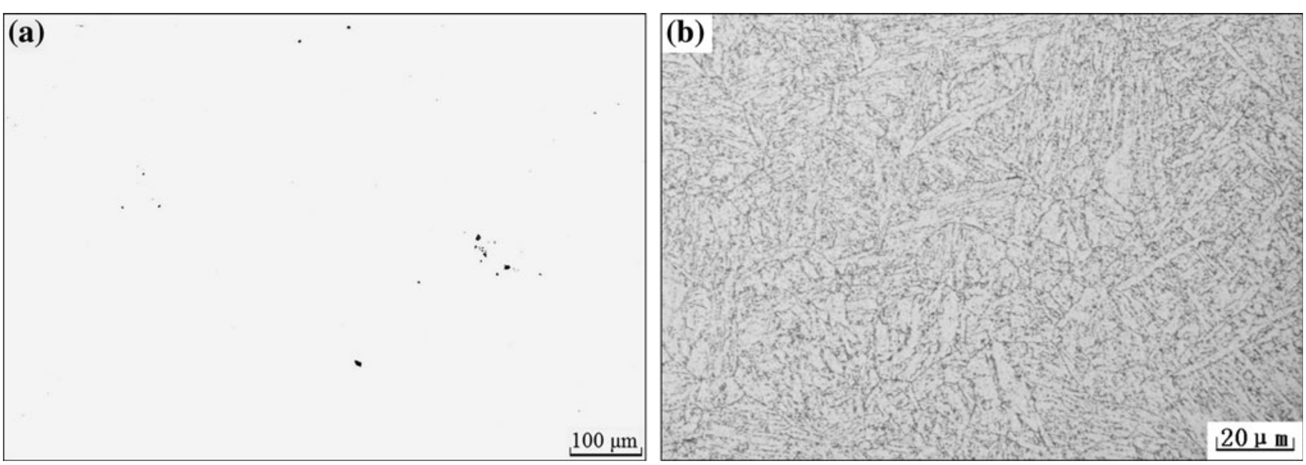

Fig. 1 Metallographic microstructures of the T91 sample (a) polished state (b) etched state

Table 2 Chemical compositions of the welding wire ER90S-B9 (wt.%)

Elements	C	Mn	Si	P	S	Ni	Cr	Mo	V	Al	Cu	Nb	N
ER90S-B9 Welding wire	0.112	0.57	0.30	0.007	0.002	0.68	9.00	0.93	0.200	0.009	0.08	0.057	0.036
ASME SFA-5.28 (AWS) ER90S-B9	0.07-0.13	≤1.25	0.15-0.30	≤0.010	≤0.010	≤1.00	8.00-9.50	0.80-1.10	0.15-0.25	≤0.04	≤0.20	0.02-0.10	0.03-0.07

Table 3 Mechanical properties of T91 welded joints at room temperature

Sample no.	Tensile strength, σ_b, MPa			Elongation, δ_5, %
	I	II	Avg.	
1	706	711	708.5	18
2	693	694	693.5	
3	707	712	709.5	
4	730	752	741.0	
5	735	721	728.0	
T91 specification	≥585			≥20

Table 4 Bending test results of T91 welded joints

Bending style	Test condition	Sample no.	Results
Face bending		1	
		2	
		3	
		4	
	$D = 3T$, $\alpha = 50°$	5	Qualified
Back bending		1	
		2	
		3	
		4	
		5	

D, denotes the bending diameter; *T*, denotes the material thickness; α, denotes the bending angle

China (Ref 40), yield strengths ($\sigma_{0.2}$) of the joints were all qualified with increase of temperatures. Also, corresponding data of the T91 welded joints with same welding wire and process from Metrode Products Ltd. (Ref 41) were listed in the table and the figure. Meanwhile, the tensile strengths of our joints at these increasing temperatures were displayed as well.

3.2 Metallographic Microstructures Inspection

Figure 3(a) displays the metallographic microstructure of the HAZ after welding, which consisted of sorbites with finer laths than that of T91 base material. Further detailedly, by means of TEM, it could be obviously observed that coarsened rod-like carbides of $M_{23}C_6$ had ripened and precipitated on the grain boundaries in the HAZ, marked with arrows in Fig. 4(a). Especially in some triangular grain boundaries, the carbides were even larger, marked in Fig. 4(b). In contrast, the weld seam was also martensite just like the T91 base material but with wider laths of about 3 μm, seen in Fig. 3(b). Moreover, tangling subgrains existed within the dislocation martensite laths (Fig. 4c), and nearly no coarsened $M_{23}C_6$ carbides had precipitated on the grain boundaries (Fig. 4d).

According to the metallographic microstructures and the TEM micrographs, compared with the weld seam, HAZ of the joints displayed fine sorbitic microstructure with coarsened $M_{23}C_6$ carbides on the grain boundaries. This could be ascribed to the heat effect from the weld seam during the welding process, thus the initial martensites decomposed into finer sorbites. Meanwhile, since carbide as $M_{23}C_6$ on the grain boundaries precipitates prior to MC within the grains (Ref 42), the $M_{23}C_6$ carbides that originally existed on the grain

Table 5 Mechanical properties of T91 welded joints at increasing temperatures

Test temperature, °C	Yield strength, $\sigma_{0.2}$, MPa			Tensile strength, σ_b, MPa
	Test results	GB 5310 specification(a)	Data from Metrode	
50	450			660
100	470	384		580
	525			650
150	475	378		590
	500			595
200		377		565
				580
250		377		560
				560
300		376		535
				530
350		371		535
				535
400		358		510
				515
450		337		480
				485
500	380	306		460
	385			455
515			490	
			540	
550	350	260		395
	365			410
575	350			375
	330			375
600	280	198		335
	290			345
625	275			310
	290			315
650	250			265
	245			280

(a) This GB 5310 specification is just for T91 base material

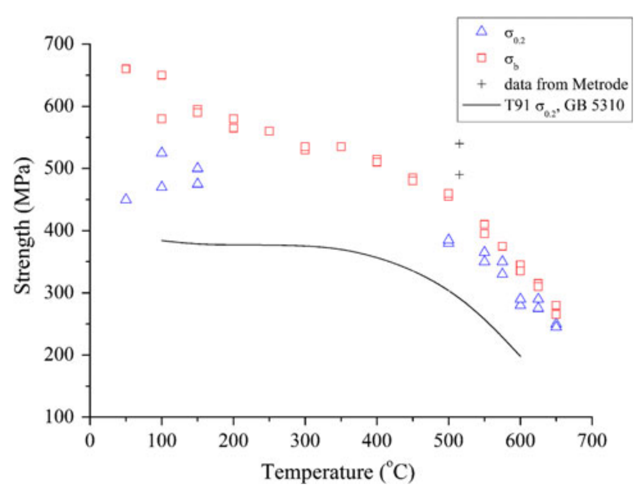

Fig. 2 Mechanical properties of T91 welded joints at increasing temperatures

boundaries for purpose of pinning strengthening ripened and turned to be coarsened under heat too. As a result, strength of the HAZ decreased and made it the weak region of the whole

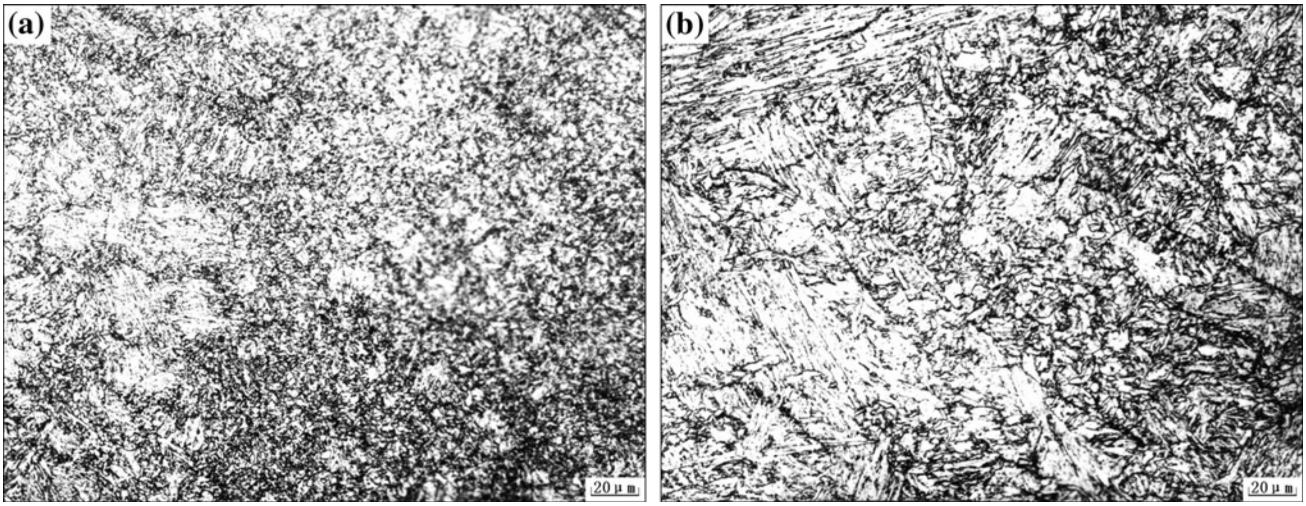

Fig. 3 Metallographic microstructures of the different regions across the T91 welded joints (a) HAZ (b) weld seam

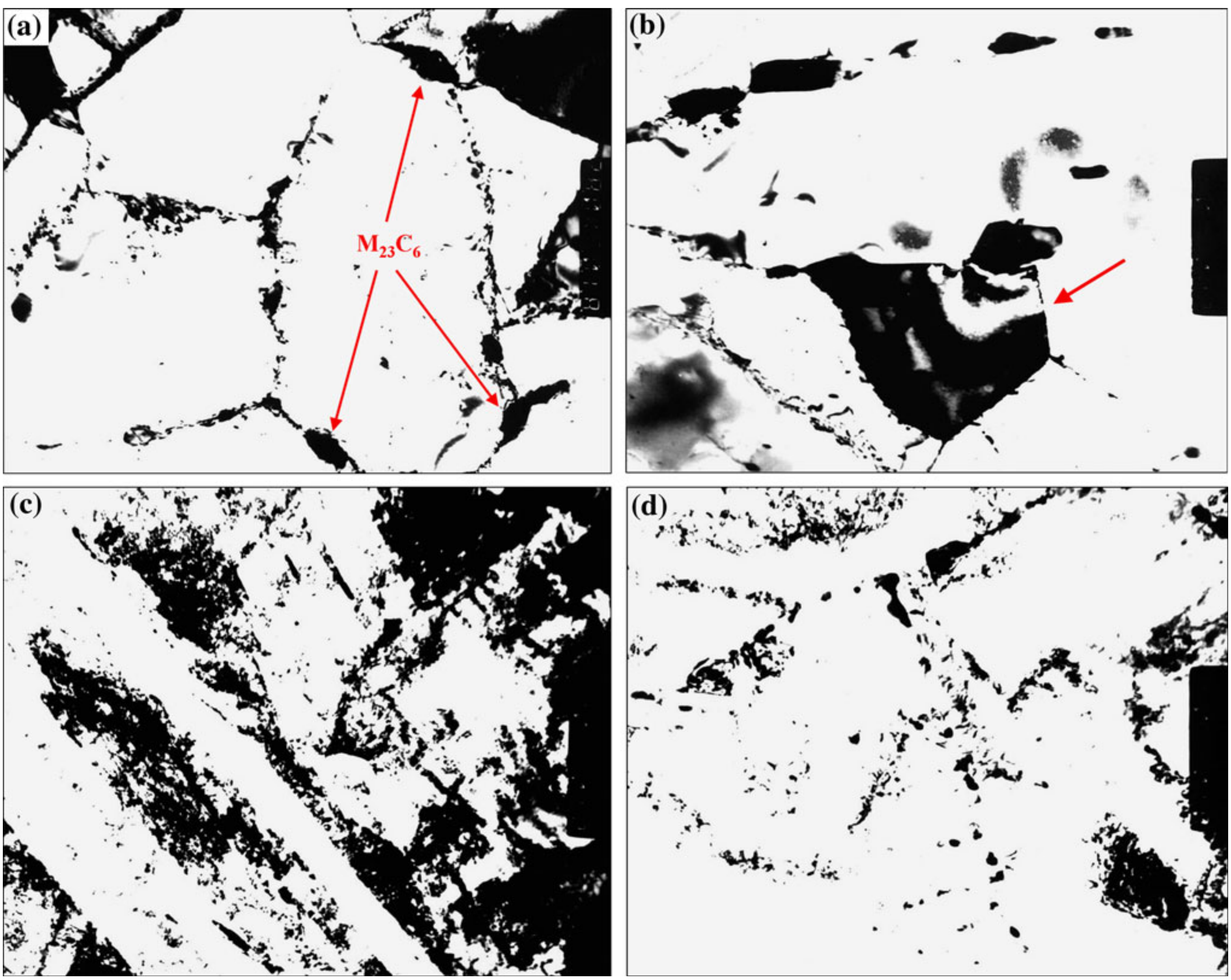

Fig. 4 TEM micrographs of the different regions across the T91 welded joints (a) HAZ, ×28,000; (b) HAZ, ×35,000; (c) weld seam, ×22,000; (d) weld seam, ×35,000

joints. However, based on the classic Ostwald ripening mechanism (Ref 43), under heat effect the precipitated carbides are first in form of rod and gradually change toward sphere with low free energy. In the present case, the rod-like $M_{23}C_6$ carbides on the grain boundaries may be regarded only in the early stage of ripening, seen in Fig. 4(a). In other words, by means of this welding and PWHT process, carbides in the HAZ did not ripen seriously and could still ensure a relatively acceptable strength for the whole welded joint. In terms of the weld seam, it underwent a complete melt-to-recrystallize procedure, therefore its grains could sufficiently grow and finally form coarser martensite laths than that of the T91 base material. What's more, the adequate welding process inhibited the $M_{23}C_6$ carbides coarsened, and consequently ensured qualified strength and toughness for the weld seam.

3.3 Aging Test

In order to investigate the performance deterioration of the T91 welded joints, aging test was carried out at 625 °C. Table 6 and Fig. 5 display the mechanical properties variation with the aging times. It can be concluded from these results that mechanical properties of the joints did not deteriorate significantly with increase of the aging time. In other words, such T91 welded joints could exhibit good structural stability at elevated temperatures.

3.4 Creep Rupture Test

Table 6 Mechanical properties of the T91 welded joints in aging test

Aging time	Yield strength, $\sigma_{0.2}$, MPa	Tensile strength, σ_b, MPa	Elongation, δ_5, %
0	450	660	18
1000	325	655	20
3000	450	680	16
5000	520	685	18
10000	495	660	15

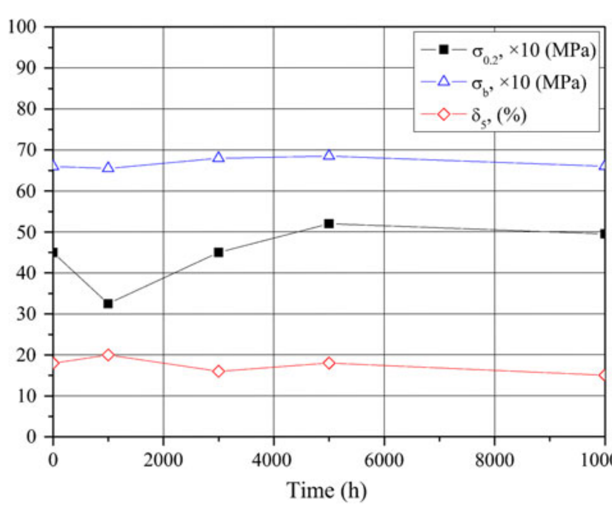

Fig. 5 Mechanical properties of the T91 welded joints in aging test

Creep rupture test was then conducted on two groups of round bar specimen of the joints at 625 °C, respectively, named Test I and Test II. Table 7 lists the rupture times under different load stresses, and their double logarithmic relationship is plotted in Fig. 6. Meanwhile, Fig. 6 also involves relevant data of the T91 welded joints at 600 °C (Ref 42), and at 550, 600, and 650 °C (Ref 30). Moreover, for purpose of comparison, the creep rupture data of the T91 base material at 625 °C (Ref 42) and our past research were both presented in Fig. 6 as well.

According to the classic equation:

$$\lg t = \lg A - B \lg \sigma \qquad \text{(Eq 1)}$$

the relationships between load stresses σ and rupture times t of the two groups of tests were both linearly fitted in Fig. 6 and mathematically expressed in Table 7. It is clearly displayed in Fig. 6 that results of the two tests well conformed

Table 7 Creep rupture test (625 °C) results of the T91 welded joints

	Rupture time, T, h		Elongation, δ_5, %	
Load stress, σ, MPa	Test I	Test II	Test I	Test II
150	33		13.1	
140	6		10.84	
130	9	95	11.16	11.9
120	266	157	11.05	10
110	113	290	13.66	6.4
105	62		13.1	
100		438.5		6
95	490	700	11.42	5.6
90	500		11.81	
80	1197	1602	3.51	6.3
75	3337		10.11	
70	1315			
65	1084		14.75	

Fitted line equation

Test I : $\lg \sigma = 2.272 - 0.120 \lg t \quad \sigma_{10^5}^{625\,°C} = 47\,\text{MPa}$
Test II : $\lg \sigma = 2.454 - 0.170 \lg t \quad \sigma_{10^5}^{625\,°C} = 40\,\text{MPa}$

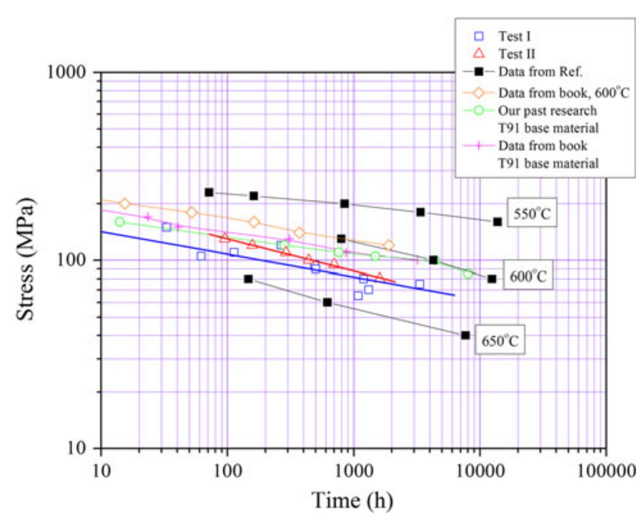

Fig. 6 Double logarithmic plot of load stress versus rupture time for the T91 welded joints at 625 °C

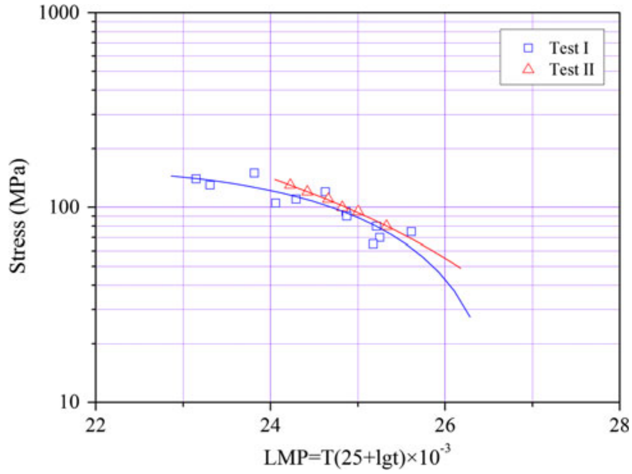

Fig. 7 Plot of stresses with LMP for the T91 welded joints

to and also supplemented the data (Ref 30) at other temperatures, but they were a bit inferior to the performance of the T91 base material at the same temperature. Furthermore, based on the two fitted lines, the threshold stresses $\sigma_{10^5}^{625\,°C}$ of the joints at 625 °C, after 10^5 h were approximately estimated: 47 and 40 MPa, already higher than the steam pressures of USC condition. If considering the safety factor, these threshold stresses should also be divided by a safety coefficient (Ref 44, 45) that ranges from 1.2 to 1.6 to obtain the permitted stresses in application. However, this is also higher than the operating pressures of most nuclear reactors presently used.

It is a common sense that Larson–Miller equation is always applied to predict service lives of components on basis of creep rupture data (Ref 46). As for T91 and its welded joints, the Larson–Miller equation is defined as:

$$\mathrm{LMP} = T(25 + \lg t) \qquad \text{(Eq 2)}$$

where LMP is the dimensionless Larson–Miller parameter, T is the absolute temperature in K, and t is the rupture time in hour (Ref 47). Then, the creep rupture data can be plotted in form of lg σ versus LMP, where LMP can be calculated by Eq 2, seen in Fig. 7. After polynomial fitting, service lives of the T91 welded joints can be easily predicted. For example, under 30 MPa and 625 °C, the service life is nearly 60,000 h; under 25 MPa and 550 °C, the upper limit operating conditions of most current nuclear reactors (Ref 48–51), the service life could be over 10^7 h. Thus, it can be concluded that this kind of China-made T91 welded joints were comprehensively qualified to be applied in nuclear power industry.

4. Conclusions

1. Mechanical properties of this China-made T91 welded joints were qualified at both room and increasing temperatures according to relevant standards. What's more, aged at 625 °C for 10,000 h, tensile properties of the joints did not exhibit obvious deterioration as well.
2. After welding, weld seam consisted of wider martensite laths than that of T91 base material, and no coarsened carbides were observed on the grain boundaries. However, HAZ of the joint changed into fine sorbites with coarsened $M_{23}C_6$ carbides precipitated on the grain boundaries, leading it the weak region of the whole joints.
3. Based on the creep rupture test, such T91 welded joints could ensure sufficient heat strength under the operating conditions of most currently used nuclear reactors. And its service life was estimated to be over 10^7 h under 25 MPa and 550 °C.

Acknowledgments

The work was supported by both National Natural Science Foundation of China (Grant 50871076) and Shanghai Leading Academic Discipline Project (Project Number: B113). Meanwhile, part of the tests was cooperated by Shanghai Institute of Special Equipment Inspection & Technical Research and Shanghai Boiler works Ltd. Finally, gratitude must also be given to Shanghai Research Institute of Materials for providing various experimental conditions.

References

1. R.L. Klueh and A.T. Nelson, Ferritic/Martensitic Steels for Next-Generation Reactors, *J. Nucl. Mater.*, 2007, **371**, p 37–52
2. J. Van den Bosch and A. Almazouzi, Compatibility of Martensitic/Austenitic Steel Welds with Liquid Lead Bismuth Eutectic Environment, *J. Nucl. Mater.*, 2009, **385**, p 504–509
3. F. Masuyama, History of Power Plants and Progress in Heat Resistant Steels, *ISIJ Int.*, 2001, **41**, p 612–625
4. R. Viswanathan and W. Bakker, Materials for Ultrasupercritical Coal Power Plants–Boiler Materials: Part 1, *J. Mater. Eng. Perform.*, 2001, **10**, p 81–95
5. J. Hansen, M. Sato, R. Ruedy, K. Lo, D.W. Lea, and M. Medina-Elizade, Global Temperature Change, *Proc. Natl. Acad. Sci. USA*, 2006, **103**, p 14288–14293
6. Y. Gong and Z.G. Yang, Corrosion Evaluation of One Dry Desulfurization Equipment—Circulating Fluidized Bed Boiler, *Mater. Des.*, 2011, **32**, p 671–681
7. J. Cao, Y. Gong, K. Zhu, Z.G. Yang et al., Microstructure and Mechanical Properties of Dissimilar Materials Joints Between T92 Martensitic and S304H Austenitic Steels, *Mater. Des.*, 2011, **32**, p 2763–2770
8. K.H. Lo, C.H. Shek, and J.K.L. Lai, Recent Developments in Stainless Steels, *Mater. Sci. Eng. R*, 2009, **65**, p 39–104
9. J. Cao, Y. Gong, Z.G. Yang et al., Creep Fracture Behavior of Dissimilar Weld Joint Between T92 Martensitic and HR3C Austenitic Steels, *Int. J. Pres. Ves. Pip.*, 2011, **88**, p 94–98
10. J.C. An, H.Y. Jing, G.C. Xiao, L. Zhao, and L.Y. Xu, Analysis of the Creep Behavior of P92 Steel Welded Joint, *J. Mater. Eng. Perform.*, 2010, doi:10.1007/s11665-010-9779-x
11. Y. Gong, J. Cao, L.N. Ji, Z.G. Yang et al., Assessment of Creep Rupture Properties for Dissimilar Steels Welded Joints Between T92 and HR3C, *Fatigue Fract. Eng. M*, 2011, **34**, p 83–96
12. A. Roy, P. Kumar, and D. Maitra, The Effect of Silicon Content on Impact Toughness of T91 Grade Steels, *J. Mater. Eng. Perform.*, 2009, **18**, p 205–210
13. C. Keller, M.M. Margulies, Z. Hadjem-Hamouche, and I. Guillot, Influence of the Temperature on the Tensile Behaviour of a Modified 9Cr–1Mo T91 Martensitic Steel, *Mater. Sci. Eng. A*, 2010, **527**, p 6758–6764
14. D. Laverde, T. Gómez-Acebo, and F. Castro, Continuous and Cyclic Oxidation of T91 Ferritic Steel Under Steam, *Corros. Sci.*, 2004, **46**, p 613–631
15. L. Nieto Hierro, V. Rohr, P.J. Ennis, M. Schütze, and W.J. Quadakkers, Steam Oxidation and Its Potential Effects on Creep Strength of Power Station Materials, *Mater. Corros.*, 2005, **56**, p 890–896

16. R. Viswanathan, J. Sarven, and J.M. Tanzosh, Boiler Materials for Ultra-Supercritical Coal Power Plants—Steamside Oxidation, *J. Mater. Eng. Perform.*, 2006, **15**, p 255–274
17. J. Čadek, V. Šustek, and M. Pahutová, An Analysis of a Set of Creep Data for a 9Cr-1Mo-0.2V (P91 type) Steel, *Mater. Sci. Eng. A*, 1997, **225**, p 22–28
18. V. Sklenička, K. Kuchařová, M. Svoboda, L. Kloc, J. Buršík, and A. Kroupa, Long-Term Creep Behavior of 9–12%Cr Power Plant Steels, *Mater. Charact.*, 2003, **51**, p 35–48
19. B. Fournier, M. Salvi, F. Dalle, Y. De Carlan, C. Caës et al., Lifetime Prediction of 9–12%Cr Martensitic Steels Subjected to Creep-Fatigue at High Temperature, *Int. J. Fatigue*, 2010, **32**, p 971–978
20. A. Kumar, K. Laha, T. Jayakumar, K. Bhanu Sankara Rao, and B. Raj, Comprehensive Microstructural Characterization in Modified 9Cr-1Mo Ferritic Steel by Ultrasonic Measurements, *Metall. Mater. Trans. A*, 2002, **33A**, p 1617–1626
21. V. Homolová, J. Janovec, P. Záhumenský, and A. Výrostková, Influence of Thermal-Deformation History on Evolution of Secondary Phases in P91 Steel, *Mater. Sci. Eng. A*, 2003, **349**, p 306–312
22. D.R.G. Mitchell and S. Sulaiman, Advanced TEM Specimen Preparation Methods for Replication of P91 Steel, *Mater. Charact.*, 2006, **56**, p 49–58
23. A.K. Roy, D. Maitra, and P. Kumar, The Role of Silicon Content on Environmental Degradations of T91 Steels, *J. Mater. Eng. Perform.*, 2008, **17**, p 612–619
24. Z. Jiao, N. Ham, and G.S. Was, Microstructure of Helium-Implanted and Proton-Irradiated T91 Ferritic/Martensitic Steel, *J. Nucl. Mater.*, 2007, **367–370**, p 440–445
25. D.C. Foley, K.T. Hartwig, S.A. Maloy, P. Hosemann, and X. Zhang, Grain Refinement of T91 Alloy by Equal Channel Angular Pressing, *J. Nucl. Mater.*, 2009, **389**, p 221–224
26. C.R. Das, S.K. Albert, A.K. Bhaduri, G. Srinivasan, and B.S. Murty, Effect of Prior Microstructure on Microstructure and Mechanical Properties of Modified 9Cr-1Mo Steel Weld Joints, *Mater. Sci. Eng. A*, 2008, **477**, p 185–192
27. M. Sireesha, K. Shaju Albert, and S. Sundaresan, Microstructure and Mechanical Properties of Weld Fusion Zones in Modified 9Cr-1Mo Steel, *J. Mater. Eng. Perform.*, 2001, **10**, p 320–330
28. A. Thomas, B. Pathiraj, and P. Veron, Feature Tests on Welded Components at Higher Temperatures—Material Performance and Residual Stress Evaluation, *Eng. Fract. Mech.*, 2007, **74**, p 969–979
29. S. Spigarelli and E. Quadrini, Analysis of the Creep Behaviour of Modified P91 (9Cr-1Mo-NbV) Welds, *Mater. Des.*, 2002, **23**, p 547–552
30. Y.K. Li, H. Hongo, M. Tabuchi, Y. Takahashi, and Y. Monma, Evaluation of Creep Damage in Heat Affected Zone of Thick Welded Joint for Mod.9Cr-1Mo Steel, *Int. J. Pres. Ves. Pip.*, 2009, **86**, p 585–592
31. T. Watanabe, M. Tabuchi, M. Yamazaki, H. Hongo, and T. Tanabe, Creep Damage Evaluation of 9Cr-1Mo-V-Nb Steel Welded Joints Showing Type IV Fracture, *Int. J. Pres. Ves. Pip.*, 2006, **83**, p 63–71
32. F. Vivier, A.F. Gourgues-Lorenzon, and J. Besson, Creep Rupture of a 9Cr1MoNbV Steel at 500°C: Base Metal and Welded Joint, *Nucl. Eng. Des.*, 2010, **240**, p 2704–2709
33. ASME SA-213M-2001, *Seamless Stainless Steel Tubes for Boiler and Heat Exchanger*, ASME, Washington, DC, 2001
34. ISO 4967-1998, Steel—Determination of Content of Nonmetallic Inclusions—Micrographic Method Using Standard Diagrams. ISO, Genève, Switzerland, 1998
35. ASME SFA-5.28M-2007, *Low-Alloy Steel Electrodes and Rods for Gas Shielded Arc Welding*, ASME, Washington, DC, 2007
36. ASTM E8-04, *Standard Test Methods for Tension Testing of Metallic Materials*, ASTM, West Conshohocken, 2004
37. ASTM E290-97a(2004), Standard Test Methods for Bend Testing of Material for Ductility, ASTM, West Conshohocken, 2004
38. ISO 783-1999, Metallic Materials—Tensile Testing at Elevated Temperature, ISO, Genève, Switzerland, 1999
39. ASTM E139-06, Standard Test Methods for Conducting Creep, Creep-Rupture, and Stress-Rupture Tests of Metallic Materials, ASTM, West Conshohocken, 2006
40. GB 5310-2008, *Seamless Steel Tubes and Pipes for High Pressure Boiler*, SAC, Beijing, 2008
41. Welding Consumables for P91 Steels for the Power Generation Industry, Metrode Products Ltd
42. G.G. Shu, J.N. Liu, C.Z. Shi, Z.P. Wang, and Y.F. Zhao, *Microstructural Properties and Engineering Applications of T/P91 Steel used in Supercritical Boilers*, Shaanxi Science & Technology Press, Xi'an, Shaanxi Province, 2006
43. W. Ostwald, *Lehrbuch der Allgemeinen Chemie, vol. 2, part 1*, Leipzig, Germany, 1896
44. Z.F. Hu and Z.G. Yang, An Investigation of the Embrittlement in X20CrMoV12.1 Power Plant Steel after Long-Term Service Exposure at Elevated Temperature, *Mater. Sci. Eng. A*, 2004, **383**, p 224–228
45. Z.F. Hu and Z.G. Yang, Identification of the Precipitates by TEM and EDS in X20CrMoV12.1 after Long-Term Service at Elevated Temperature, *J. Mater. Eng. Perform.*, 2003, **12**, p 106–111
46. F.R. Larson and J. Miller, A Time-Temperature Relationship for Rupture and Creep Stresses, *Trans. ASME*, 1952, **74**, p 765–775
47. D. Jandová, J. Kasl, and V. Kanta, Creep Resistance of Similar and Dissimilar Weld Joints of P91 Steel, *Mater. High. Temp.*, 2006, **23**, p 165–170
48. M.M. Abu-Khader, Recent Advances in Nuclear Power: A Review, *Prog. Nucl. Energ.*, 2009, **51**, p 225–235
49. D.T. Ingersoll, Deliberately Small Reactors and the Second Nuclear Era, *Prog. Nucl. Energ.*, 2009, **51**, p 589–603
50. M. Lenzen, Life Cycle Energy and Greenhouse Gas Emissions of Nuclear Energy: A Review, *Energ. Convers. Manage.*, 2008, **49**, p 2178–2199
51. M. Piera, A. Lafuente, A. Abánades, and J.M. Martinez-Val, Hybrid Reactors: Nuclear Breeding or Energy Production?, *Energ. Convers. Manage.*, 2010, **51**, p 1758–1763